# Corrosion-Protection Aspects of Electrochemically Synthesized Poly(*o*-anisidine) Coatings on Mild Steel: An Electrochemical Impedance Spectroscopy Study

**Sudeshna Chaudhari, P. P. Patil**

*Department of Physics, North Maharashtra University, Jalgaon 425 001, Maharashtra, India*

Received 22 May 2006; accepted 6 March 2007
DOI 10.1002/app.26485
Published online 21 June 2007 in Wiley InterScience (www.interscience.wiley.com).

**ABSTRACT:** The corrosion-protection aspects of poly(*o*-anisidine) (POA) coatings on mild steel in aqueous 3% NaCl solutions were investigated with electrochemical impedance spectroscopy, a potentiodynamic polarization technique, and open circuit potential measurements. The POA coatings were electrochemically synthesized on mild steel with cyclic voltammetry from an aqueous salicylate medium. The corrosion behavior of the POA coatings was investigated through immersion tests performed in aqueous 3% NaCl solutions, and the recorded electrochemical impedance spectra were fitted with an equivalent circuit to obtain the characteristic impedance parameters. The use of a single equivalent circuit was inadequate to explain the various physical and electrochemical processes occurring at different exposure times. It was suggested that some characteristic element(s) should be incorporated into the equivalent circuit at different stages of the immersion to elucidate the various processes occurring at different exposure times. The evolution of the impedance parameters with the immersion time was studied, and the results showed that POA acted as a protective coating on the mild steel against corrosion in a 3% NaCl solution. From these data, the water uptake and delamination area were determined to further support the corrosion-protection performance of the POA coating. © 2007 Wiley Periodicals, Inc. J Appl Polym Sci 106: 400–410, 2007

**Key words:** coatings; conducting polymers

## INTRODUCTION

During the last 2 decades and even now, conducting polymers have continued to be the focus of active research in many technological areas such as rechargeable batteries,[1,2] sensors,[3,4] electromagnetic interference shielding,[5,6] electrochromic display devices,[7,8] smart windows,[9] molecular devices,[10] energy storage systems,[11] and membrane gas separation[12] because of their remarkable physical attributes.[1–6] The use of conducting polymers as advanced coating materials for the corrosion protection of oxidizable metals has become one of the most exciting new research fields in recent times.[13–18] Deberry[19] was the first to show that electrochemically synthesized polyaniline acts as a corrosion-protective layer on stainless steel in 1*M* $H_2SO_4$. Since then, several research groups[20–24] have systematically investigated the performance of various conducting polymers as corrosion-protective coatings on oxidizable metals. In those investigations, electrochemical techniques such as potentiodynamic polarization measurements, cyclic polarization measurements, open circuit potential measurements, and electrochemical impedance spectroscopy (EIS) have been used to evaluate the corrosion-protection performance of the conducting-polymer coatings. Among the electrochemical techniques, EIS is a rapid and convenient technique for evaluating the performance of coatings applied to oxidizable metals.

Several researchers[25–29] have used EIS to investigate the corrosion protection of oxidizable metals by conducting-polymer coatings. They have modeled the impedance plots of conducting-polymer-coated metals, using electrical equivalent circuits, and obtained various electrochemical impedance parameters.

The incorporation of constituents into the polymer skeleton is a common technique for synthesizing polymers with improved properties. This concept has been successfully applied to polyaniline.[30,31] Considerable work is still needed to understand the basic issues related to the electrodeposition of substituted polyanilines on oxidizable metals and to explore the possibility of using them as alternatives to polyaniline for the corrosion protection of metals.

In this article, we report an EIS study on the corrosion protection of mild steel by poly(*o*-anisidine) (POA) coatings. The corrosion-protection properties of the POA coatings were investigated through

*Correspondence to:* P. P. Patil (pnmu@yahoo.co.in).
Contract grant sponsor: University Grants Commission (New Delhi, India; through the Special Assistance Programme at Department Research Support Level program).
Contract grant sponsor: Department of Atomic Energy, Board of Research in Nuclear Sciences (Mumbai, India).

immersion tests performed in 3% NaCl solutions, and the recorded impedance spectra were analyzed in terms of the evolution of the characteristic impedance parameters with the immersion time. The objectives of this study were (1) to evaluate the performance of POA as a protective coating against the corrosion of mild steel in aqueous 3% NaCl solutions by EIS, (2) to study the evolution of an equivalent circuit with the immersion time to analyze the spectra recorded as a function of the immersion time, and (3) to examine the possibility of using POA coatings for the corrosion protection of mild steel in aqueous 3% NaCl.

The choice of *o*-anisidine as the monomer for this study was based on the following:

1. *o*-Anisidine is a substituted derivative of aniline with a methoxy (—$OCH_3$) group substituted at the ortho position, and so this study explores the possibility of using POA as an alternative to polyaniline for the corrosion protection of mild steel.
2. The monomer *o*-anisidine is commercially available at a low cost.
3. The *o*-anisidine monomer has quite good solubility in water, and so the electrochemical synthesis of POA from an aqueous bath may provide an alternative for reducing the use of hazardous chemicals as well as the cost of waste disposal.
4. The conversion of the monomer to the polymer is a straightforward process.

## EXPERIMENTAL

Analytical-reagent-grade chemicals were used throughout this study. The *o*-anisidine monomer was double-distilled before its use. An aqueous sodium salicylate ($NaC_7H_5O_3$) solution was used as the supporting electrolyte. The concentrations of $NaC_7H_5O_3$ and *o*-anisidine were kept constant at 0.1*M* each.

The chemical composition of the mild steel used in this study was as follows: 0.03 wt % C, 0.026 wt % S, 0.01 wt % P, 0.002 wt % Si, 0.04 wt % Ni, 0.002 wt % Mo, 0.16 wt % Mn, 0.093 wt % Cu, and 99.64 wt % Fe. The mild steel substrates ($\sim$ 10 mm $\times$ 15 mm $\times$ 0.5 mm) were polished with a series of emery papers, and this was followed by thorough rinsing in acetone and double-distilled water and drying in air. Before any experiment, the substrates were treated as described and freshly used with no further storage.

In this work, the POA coatings were synthesized through the electrochemical polymerization of *o*-anisidine on mild steel substrates from an aqueous salicylate solution through cyclic voltammetry. The electrochemical polymerization was carried out in a single-compartment, three-electrode cell with steel as a working electrode (150 $mm^2$), platinum as a counter electrode, and a saturated calomel electrode (SCE) as a reference electrode. The cyclic voltammetry conditions were maintained with an electrochemical measurement system (SI 1280B, Solartron, Hampshire, UK) controlled by corrosion software (CorrWare electrochemistry/corrosion software, Scribner Associates, supplied by Solartron). The synthesis was carried out by continuous cycling of the electrode potential between $-1.0$ V and 1.8 V at a potential scan rate of 0.02 V/s. After deposition, the working electrode was removed from the electrolyte, rinsed with double-distilled water, and dried in air. The thickness of the coatings was determined by a conventional magnetic-induction-based, microprocessor-controlled coating thickness gauge (Minitest 600, ElectroPhysik, Germany). The error in the thickness measurements was less than 5%.

Scanning electron microscopy (SEM) was employed to characterize the surface morphology with a Leica Cambridge (Cambridge, UK) 440 microscope.

The corrosion-protection performance of the POA coatings was investigated in an aqueous 3% NaCl solution with open circuit potential measurements, a potentiodynamic polarization technique, and EIS. For these measurements, a Teflon holder was used to encase the polymer-coated mild steel substrates so as to leave an area of $\sim$ 40 $mm^2$ exposed to the solution. The substrates were allowed to stabilize in the electrolyte for 30 min before the potentiodynamic polarization and EIS measurements. The EIS measurements of the POA-coated mild steel were carried out at the open circuit potential in an aqueous 3% NaCl solution. The frequency was varied from 1 mHz to 20 kHz with an alternating-current excitation potential of 10 mV. The analysis of the impedance spectra was performed through the fitting of the experimental results to equivalent circuits with Z-View software from Scribner Associates.[32] The quality of the fitting to the equivalent circuit was judged first by the $\chi^2$ value, that is, the sum of the square of the differences between the theoretical and experimental points, and second by the limitation of the relative error in the value of each element in the equivalent circuit to 5%.

The potentiodynamic polarization measurements were performed by the sweeping of the potential between $-0.25$ V and 0.25 V from the open circuit potential at the scan rate of 0.002 V/s. The potentiodynamic polarization curves were analyzed with Corr-View software from Scribner Associates.[33] This software performed the Tafel fitting and calculated the values of the corrosion potential ($E_{corr}$), corrosion current density ($j_{corr}$), and corrosion rate [CR (mm/

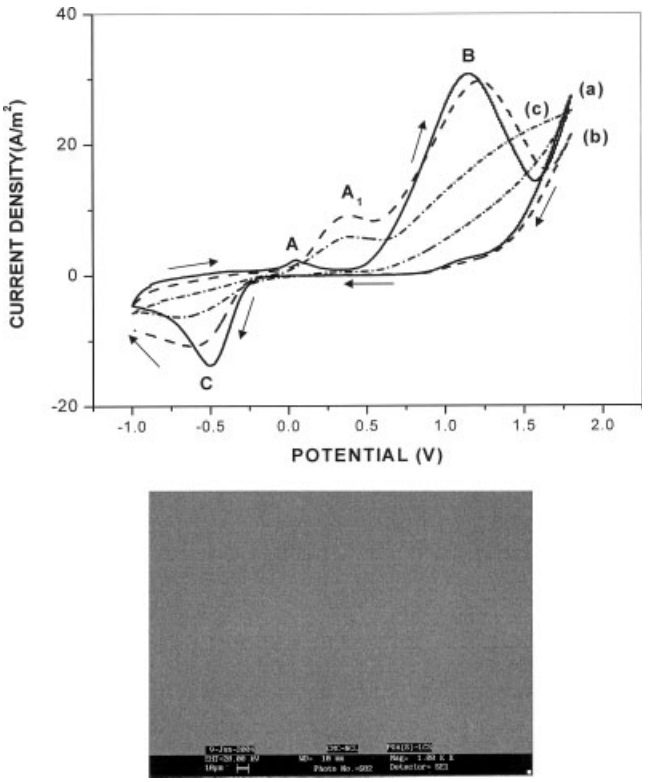


**Figure 1** Cyclic voltammograms of (a) the first, (b) second, and (c) tenth scans recorded during the synthesis of POA coatings on mild steel in 0.1*M* $NaC_7H_5O_3$ solutions. The scan rate was 0.02 V/s. An SEM image of the POA coating on mild steel is shown below the cyclic voltammograms.

year)]. All the measurements were repeated at least four times, and good reproducibility of the results was observed.

## RESULTS AND DISCUSSION

The cyclic voltammograms of the first, second, and tenth scans recorded during the synthesis of the POA coating on the mild steel electrode from an aqueous solution containing 0.1*M* *o*-anisidine and 0.1*M* $NaC_7H_5O_3$ are shown in Figure 1. The first positive cycle is characterized by (1) a small anodic peak (A) at $\sim$ 0.038 V versus SCE and (2) the onset of an oxidation wave at $\sim$ 0.469 V versus SCE followed by the oxidation peak (B) at $\sim$ 1.152 V versus SCE. During the reverse cycle, the anodic current density decreases rapidly, and a negligibly small current density can be observed until $-0.161$ V versus SCE. The negative cycle terminates with a broad reduction peak (C) at $-0.499$ V versus SCE.

The small anodic peak (A) may be attributed to the formation of iron oxides and/or to some iron salicylate compound. This passive layer reduces the further dissolution of the mild steel without preventing the electrochemical polymerization of *o*-anisidine and allows the deposition of the adherent POA film. The oxidation peak (B) at $\sim$ 1.152 V versus SCE can be attributed to the oxidation of *o*-anisidine because a black, uniform film is generated on the mild steel substrate. The reduction peak observed at $\sim -0.499$ V during the negative cycle can be attributed to the partial reduction of the deposited POA film.

During the second scan [Fig. 1(b)], the anodic peak (A) cannot be observed. In addition, a new broad anodic peak ($A_1$) at $\sim$ 0.377 V versus SCE can be observed, which is assigned to the oxidation of POA deposited at the mild steel surface corresponding to the conversion of amine units into radical cations.[34] On repetitive cycling, voltammograms identical to those of second scan can be obtained. However, the current density corresponding to the anodic peaks increases gradually with the number of scans. After the fourth scan, the cyclic voltammogram does not show well-defined redox peaks. A typical tenth scan is also shown in Figure 1(c).

An SEM image of POA ($\sim$ 6 μm thick) deposited on mild steel is also shown in Figure 1. It clearly reveals that the coating is uniform, crack, free and featureless.

The evolution of the open circuit potential for the POA-coated mild steel as a function of the immersion time in aqueous 3% NaCl was studied. The open circuit potential/time curve recorded in aqueous 3% NaCl for POA coatings electrosynthesized on mild steel under cyclic voltammetry conditions is presented in Figure 2. In this figure, the discontinuous line parallel to the time axis at $-0.710$ V represents $E_{corr}$ of uncoated mild steel.

The initial value of the open circuit potential of the POA-coated ($\sim$ 6 μm thick) mild steel was measured to be $\sim -0.440$ V versus SCE, and it is more positive than that of the uncoated mild steel by up

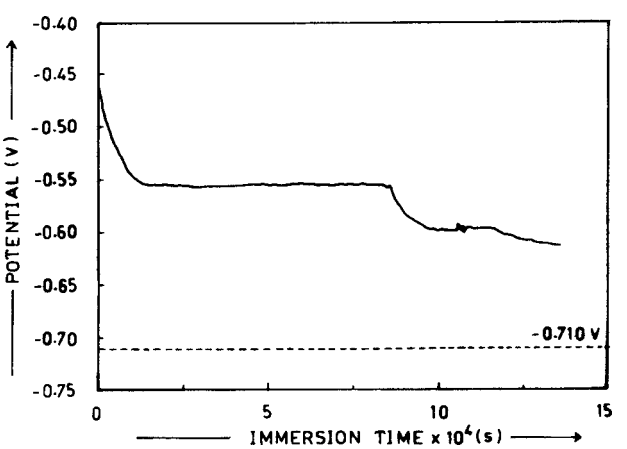


**Figure 2** Open circuit potential/time curve recorded for POA-coated mild steel (synthesized under cyclic voltammetry conditions) in aqueous 3% NaCl. The discontinuous line represents the open circuit potential of uncoated mild steel.

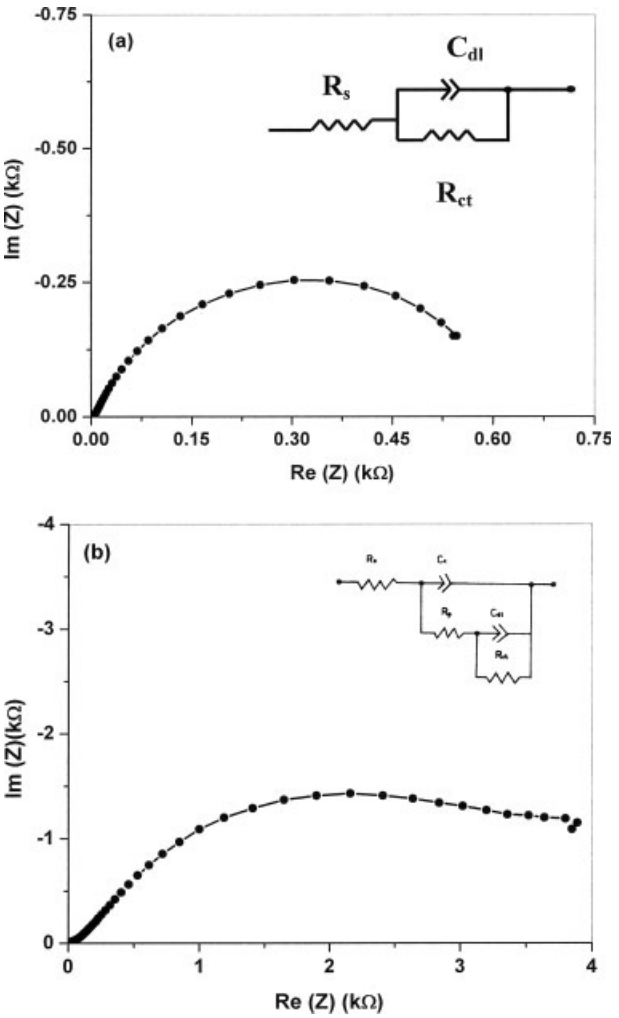


**Figure 3** Nyquist impedance plots for (a) uncoated mild steel and (b) POA-coated mild steel. The plots were recorded at the open circuit potential in aqueous solutions of 3% NaCl. The insets depict the electrical equivalent circuits used to model the impedance plots.

to ~ 0.270 V versus SCE. In the early stages of the immersion, the open circuit potential decreases sharply to −0.553 V versus SCE, and this may be due to the initiation of the water-uptake process in the coating. During the first 5 h of immersion, the open circuit potential attains a plateau, and it remains fairly constant at ~ −0.553 V versus SCE. This plateau can be observed for 24 h, during which the open circuit potential remains fairly constant at ~ −0.553 V versus SCE. During this immersion period, the POA coating exhibits barrier behavior by limiting the diffusion of the corrosive species toward the underlying mild steel substrate. After 24 h of immersion, the open circuit potential decreases to −0.612 V versus SCE, which is close to $E_{corr}$ of the uncoated mild steel; thereafter, it is no longer protected.

The Nyquist impedance plots of uncoated mild steel and POA-coated mild steel recorded in an aqueous 3% NaCl solution are shown in Figure 3. The Nyquist impedance plot of the uncoated mild steel [Fig. 3(a)] is modeled by the electrical equivalent circuit depicted in the inset of Figure 3(a), which consists of the electrolyte resistance ($R_s$), charge-transfer resistance ($R_{ct}$), and double-layer capacitance ($C_{dl}$). Thus, the impedance plot of the uncoated mild steel can be fitted with a semicircle, and this is attributed to the processes occurring at the steel surface.

The Nyquist impedance plot of POA-coated mild steel recorded in an aqueous 3% NaCl solution is shown in Figure 3(b). The electrical equivalent circuit, model A, depicted in the inset of Figure 3(b), as suggested by Fenelon and Breslin[25] was used to model the impedance plot of the POA-coated mild steel. It consists of $R_s$, the pore resistance ($R_p$), the coating capacitance ($C_c$), $R_{ct}$, and $C_{dl}$. The constant phase element (CPE) was used instead of the capacitance. The CPE represents the deviation from the true capacitance behavior. Thus, the impedance plot of POA-coated mild steel [Fig. 3(b)] can be fitted with two semicircles, a smaller one at a high frequency range followed by a larger one at lower frequencies. The first semicircle is attributed to the characteristics of the POA/electrolyte interface and is characterized by $R_p$ and $C_c$.[25–28] The second semicircle in the low-frequency region is attributed to the POA/mild steel interface, and it is characterized by $R_{ct}$ for the charge-transfer reactions occurring at the bottom of the pores in the coating and $C_{dl}$.[25–28] The values of the impedance parameters of the best fit to the experimental impedance plots for uncoated mild steel and POA-coated mild steel with the equivalent circuits shown in Figure 3(a,b) are given in Table I.

The $R_{ct}$ value is approximately 4.562 kΩ, which is about 7 times higher than that of uncoated mild steel. The higher value of $R_{ct}$ is attributed to the effective barrier behavior of the POA coating.[35] The lower values of $C_c$ and $C_{dl}$ for the POA-coated mild

**TABLE I**
**Impedance Parameter Values Extracted from the Fit to the Equivalent Circuit for the Impedance Spectra Recorded in Aqueous 3% NaCl Solutions**

| Sample | $R_s$ (Ω) | $R_p$ (Ω) | $C_c$ (F/m) | $R_{ct}$ (Ω) | $C_{dl}$ (F/m) |
|---|---|---|---|---|---|
| Bare mild steel | 5.76 | — | — | 654.3 | $7.998 \times 10^{-4}$ |
| POA-coated mild steel (~ 6 μm thick) | 34.4 | 125 | $1.832 \times 10^{-5}$ | 4562 | $5.3071 \times 10^{-5}$ |

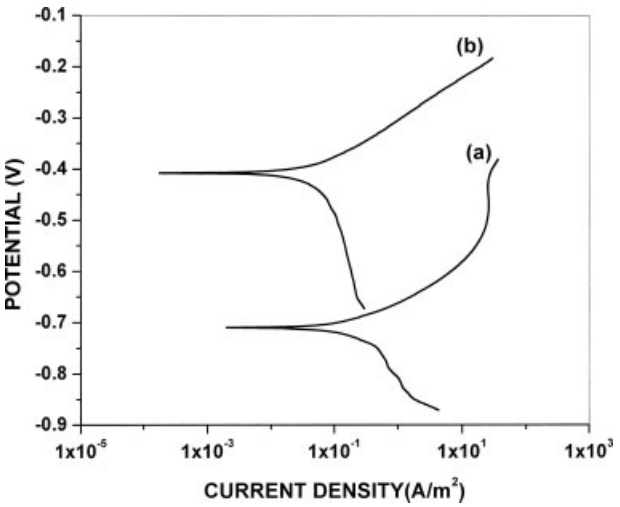


**Figure 4** Potentiodynamic polarization curves for (a) uncoated mild steel and (b) POA-coated (~ 6 μm thick) mild steel in an aqueous 3% NaCl solution.

steel provide further support for the protection of mild steel by the POA coating. Thus, the higher values of $R_{ct}$ and $R_p$ and lower values of $C_c$ and $C_{dl}$ indicate the excellent corrosion performance of the POA coating. The protection efficiency (PE) was calculated with the following expression:

$$\mathrm{PE}(\%) = \left[\frac{\mathrm{R_{pol}(coated)} - \mathrm{R_{pol}(uncoated)}}{\mathrm{R_{pol}(coated)}}\right] \times 100$$

where $R_{pol}$(uncoated) and $R_{pol}$(coated) denote the polarization resistances (for the coating polarization resistance, $R_{pol} = R_p + R_{ct}$) for uncoated and coated mild steel. The PE value calculated from the EIS data is ~ 86.04%.

The corrosion-protection performance of the POA coatings was also investigated with potentiodynamic polarization measurements. The potentiodynamic polarization curves for uncoated mild steel and POA-coated mild steel recorded in aqueous 3% NaCl are shown in Figure 4. The Tafel extrapolations show that POA caused a remarkable potential shift of ~ 0.302 V in $E_{corr}$ with respect to the value of the uncoated mild steel (−0.710 V). The positive shift in $E_{corr}$ confirms the best protection of the mild steel when its surface is covered by POA. The Tafel extrapolations were used to obtain $j_{corr}$ and thus to calculate the CR. These measurements clearly show that a substantial reduction in $j_{corr}$ occurs for the POA-coated mild steel with respect to the uncoated mild steel. The CR of POA-coated mild steel is ~ 0.03 mm/year, which is ~ 11.6 times lower than that observed for bare mild steel. The values of $E_{corr}$, $j_{corr}$, the Tafel constants ($\beta_a$ and $\beta_c$), $R_{pol}$, and CR obtained from the polarization curves are given in Table II. PE was calculated with the following expression:[28]

$$\mathrm{PE}(\%) = \left[\frac{R_{pc} - R_p}{R_{pc}}\right] \times 100$$

where $R_p$ and $R_{pc}$ denote the polarization resistances of uncoated mild steel and POA-coated mild steel, respectively. The PE value calculated from the potentiodynamic polarization data is ~ 85.37%, which is in fairly good agreement with the EIS results. Thus, these results reveal the capability of POA to act as a corrosion-protective layer on mild steel.

To gain further insight into the corrosion-protection properties of the POA coating, the impedance plots were recorded as a function of the immersion time in aqueous 3% NaCl. The Nyquist impedance plots for POA-coated mild steel recorded at different exposure times during the immersion in aqueous 3% NaCl are shown in Figure 5(a–e). These impedance plots exhibit systematic variations in terms of the values of the impedance parameters, which are the results of the changes in the dielectric characteristics of the coating due to electrolyte penetration through the pores in the coating and, consequently, the onset of corrosive processes at the surface of the mild steel substrate. Several researchers have used a single equivalent circuit model to analyze the impedance plots recorded at different times of exposure of the coating to the corrosive solution. For example, Kousik et al.[36] investigated the corrosion protection of mild steel by polythiophene coatings, using EIS. They used a single equivalent circuit model to analyze the impedance plots recorded at three different times of exposure of the coating to the corrosive solution. Recently, Zhang and Zeng[37] studied the evolution of impedance models with the immersion time for polypropylene-coated mild steel in 3.5% NaCl solution. It was shown that the number of time constants in the equivalent circuit increased with the immersion time.

When the polymer-coated metal is immersed in the corrosive electrolyte, the various physical and electrochemical processes, such as the electrolyte penetration

**TABLE II**
**Potentiodynamic Polarization Measurement Results**

| Sample | $E_{corr}$ (V) | $j_{corr}$ (A/m$^2$) | $\beta_a$ (V/dec) | $\beta_c$ (V/dec) | $R_{pol}$ (Ω/m$^2$) | CR (mm/year) |
|---|---|---|---|---|---|---|
| Uncoated mild steel | −0.710 | 30.71 | 0.084 | 0.185 | $821.72 \times 10^4$ | 0.35 |
| POA-coated mild steel (~ 6 μm thick) | −0.404 | 0.002988 | 0.054 | 0.136 | $5616.98 \times 10^4$ | 0.034 |

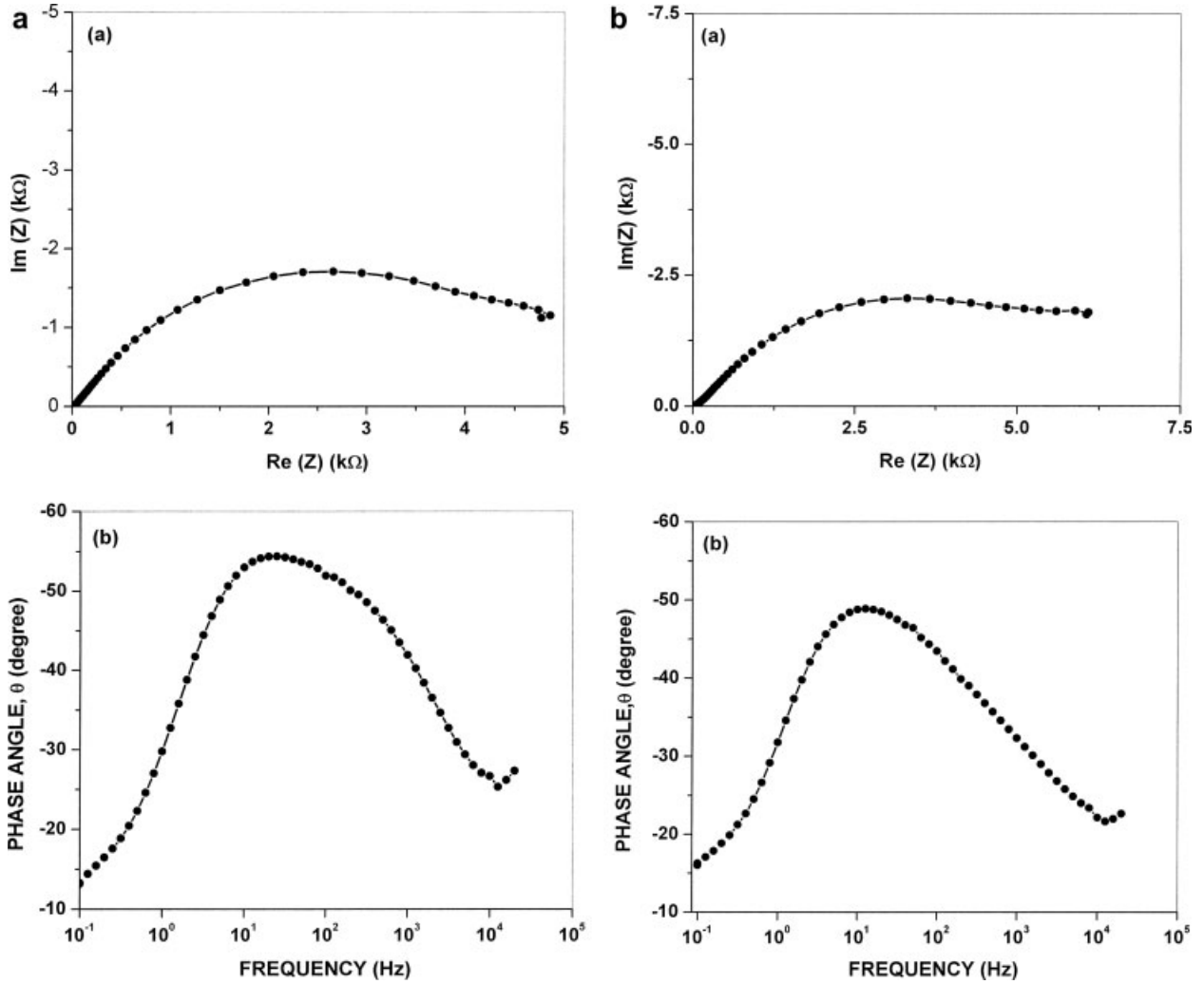


**Figure 5** Nyquist impedance plots for POA-coated (~ 6 μm thick) mild steel recorded (a) after 2 h of immersion in 3% NaCl (the corresponding Bode plot is shown below the Nyquist impedance plot), (b) after 4 h of immersion in 3% NaCl (the corresponding Bode plot is shown below the Nyquist impedance plot), (c) after 16 h of immersion in 3% NaCl (the inset depicts model B, and the corresponding Bode plots fitted with electrical equivalent circuit models A and B are shown below the Nyquist impedance plot), (d) after 48 h of immersion in 3% NaCl, and (e) after 72 h of immersion in 3% NaCl.

and/or diffusion in the coating, water uptake, onset of corrosive processes at the surface of the metal, formation and diffusion of corrosion products, and detachment of the coating, occur at different exposure times. Consequently, the use of a single equivalent circuit model at all immersion times is inadequate to explain the various aforementioned processes. Hence, it is expected that some characteristic element(s) corresponding to the various aforementioned processes should be incorporated into the equivalent circuit model at different stages of immersion. This implies that the time evolution of the equivalent circuit model should be taken into consideration during the analysis of the impedance plots recorded as a function of the immersion time. In this work, to analyze the impedance plots for POA-coated mild steel recorded at different exposure times during the immersion in aqueous 3% NaCl, two different equivalent circuit models were employed at two subsequent stages of the immersion.

### Immersion time (2–4 h)

The Nyquist impedance plot recorded at 2 h of exposure time during the immersion in an aqueous 3% NaCl solution is shown in Figure 5(a). This plot was analyzed in terms of the same equivalent circuit model (A) shown in the inset of Figure 3(b). It is fitted with two semicircles with diameters $R_p$ (at a higher frequency range) and $R_{ct}$ (at lower frequencies). $R_p$ is related to the penetration of the electrolyte into the micropores of the coating.[38] It usually

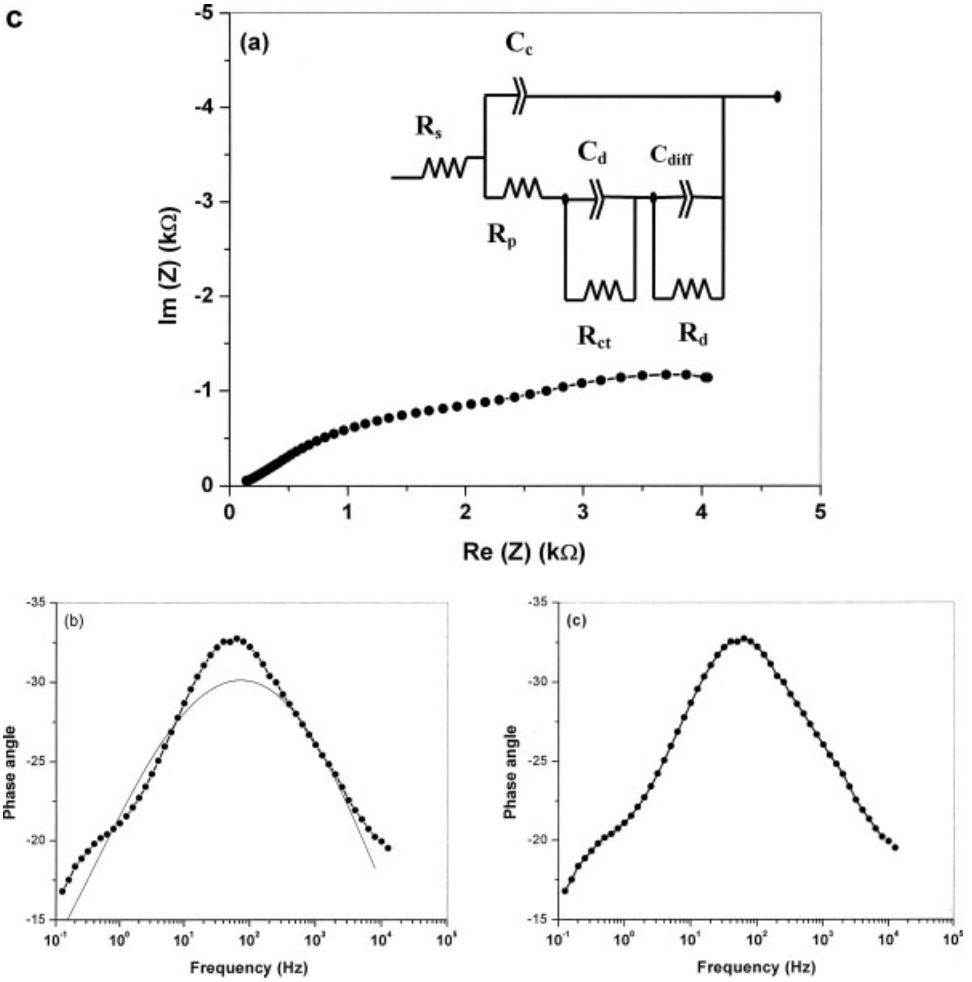


**Figure 5** *(Continued from the previous page)*

decreases with the time of exposure of the coating to the electrolyte. $R_{ct}$ is related to the corrosion processes occurring at the metal substrate beneath the coating. The $R_{ct}$ value increases during this immersion period, and this is attributed to the oxidation of the mild steel by the conducting polymer, which results in the formation of iron oxide compounds at the POA/mild steel interface and also in the partial reduction of the polymer film. The $R_p$ value decreases slightly during this immersion time. The slight decrease in the value of $R_p$ is attributed to the entry of the electrolyte into the micropores in the coating.

It is known that the phase angle is more sensitive to the state change of both the coating and metal surface. The phase angle/frequency Bode curve recorded for POA-coated mild steel after 2 h of exposure during immersion in an aqueous 3% NaCl solution is shown in Figure 5(a). The value of the phase angle is maximum ($\sim 55^\circ$) at the middle frequencies and then decreases sharply to $\sim 13^\circ$ at the lowest frequency. This observation provides evidence for limited diffusability through the POA coating.

The Nyquist impedance plot recorded after 4 h of exposure during the immersion in an aqueous 3% NaCl solution is shown in Figure 5(b). This impedance plot is also fitted satisfactorily to equivalent circuit model A, as shown in the inset of Figure 3(b). The $R_{ct}$ value increases further, whereas $R_p$ decreases further, during this immersion time. The increase in the $R_{ct}$ value may be attributed to the further reduction of the polymer film and formation of the thicker layer of the protective iron oxide compounds. The decrease in the value of $R_p$ is attributed to the entry of the electrolyte into the pores in the coating. The $E_{corr}$ value at this immersion time was measured to be $-0.400$ V versus SCE and is more positive than that of $E_{corr}$ for the uncoated mild steel by up to 0.310 V. Therefore, it can be said that during the first 4 h of immersion, the detectable corrosion processes were not started at the mild steel substrate surface under the coating.

The phase angle/frequency Bode curve recorded for POA-coated mild steel after 4 h of exposure [Fig. 5(b)] is similar to that observed after 2 h of exposure. This suggests that the POA coating has limited

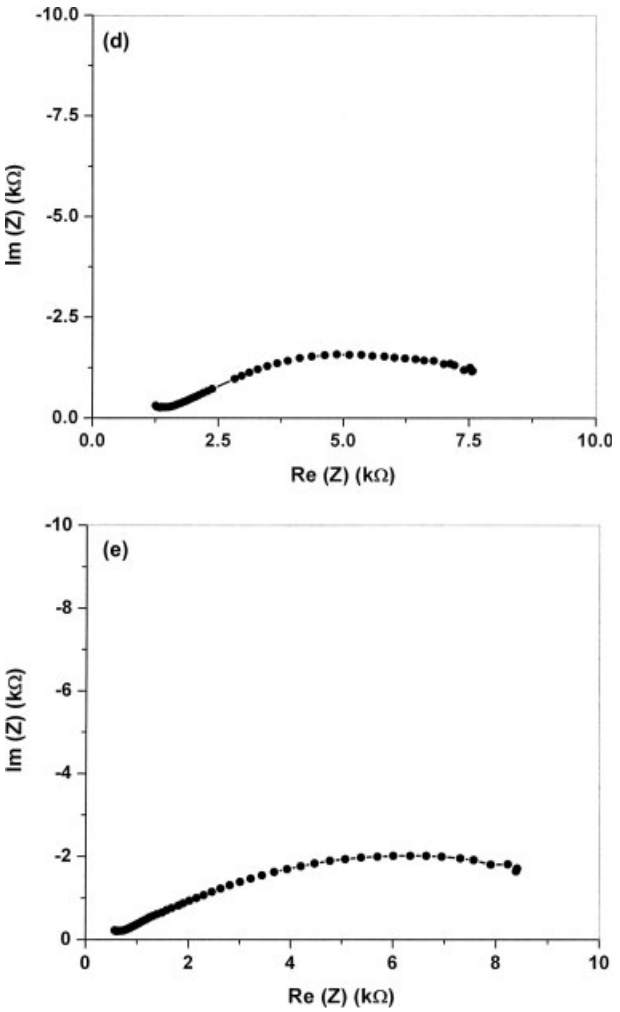


**Figure 5** (*Continued from the previous page*)

diffusability for corrosive species even after 4 h of immersion.

### Immersion time (16–72 h)

Further increasing the exposure time does not result in an obvious variation in the shape of the Nyquist impedance plots. The Nyquist impedance plot for the POA-coated mild steel recorded after 16 h of exposure during immersion in an aqueous 3% NaCl solution is shown in Figure 5(c). As seen earlier, the Nyquist impedance plots before 16 h of immersion are fitted satisfactorily to equivalent circuit model A. However, the experimental Nyquist impedance plot after 16 h of immersion cannot be well fitted to model A. The validity of the selected equivalent circuit model can be verified by a comparison of the fitness of the fitted curve to the experimental Bode curve with two different circuit models. The experimental Bode curve [Fig. 5(c)] cannot be satisfactorily fitted to model A; the fitting curve is not in agreement with the experimental data at the intermediate and low frequencies.

The electrolyte penetrates via the pores in the coating and develops the electrolyte pathways with time through the coating. The corrosive species along with the water diffuse through these paths toward the mild steel surface. When a sufficient amount of the electrolyte reaches the mils steel surface, the corrosion processes are initiated at the POA/mild steel interface. As a result, the $E_{corr}$ value shifts to a less noble value. The measured open circuit potential value at this moment is $\sim -0.550$ V versus SCE. Therefore, it can be said that after 16 h of immersion, the anodic dissolution of the passive oxide layer begins at the bottom of the pores; it interacts with the electrolyte solution and results in the formation of corrosion products that diffuse toward the coating surface through the pores in the coating.

Therefore, it is expected that the characteristic element(s) would appear in the equivalent circuit, which corresponds to the diffusion of corrosion products from the mild steel surface toward the coating. A diffusion combination, which consists of the diffusion resistance ($R_{diff}$) and the diffusion capacitance ($C_{diff}$), must be considered in the equivalent circuit. The corresponding equivalent circuit, model B, is shown in the inset of Figure 5(c) and consists of three time constants. Obviously, the first time constant is a representative of the characteristics of the POA coating. The second and third capacitive loops are attributed to the complex reactions occurring at the surface of the mild steel substrate. The second loop is determined by $R_{ct}$ and by $C_{dl}$, and the third loop is correlated to diffusion processes ($R_{diff}$ and $C_{diff}$) caused by the presence of corrosion products. The fitting curve gives a good fit to the experimental Bode curve [Fig. 5(c)] when equivalent circuit model B [as shown in the inset of Fig. 5(c)] is used. In the following immersion times, the equivalent circuit basically remains unchanged until the test is terminated.

After 16 h of immersion, the $R_{ct}$ value decreases, and its value is $\sim 5.539$ kΩ. The decrease in the value of $R_{ct}$ may be due to the dissolution of the passive oxide layer on the mild steel surface. $R_{diff}$ is the resistance against the diffusion of the corrosion products from the mild steel surface toward the coating, and its value is 3.526 kΩ.

The Nyquist impedance plot recorded after 48 h of exposure during immersion in an aqueous 3% NaCl solution is shown in Figure 5(d). Equivalent circuit model B [as shown in the inset of Fig. 5(c)] is used to fit the experimental data. After 48 h of immersion, the $R_{ct}$ value decreases further to 4.873 kΩ. However, it is higher than that of the uncoated mild steel. The $R_{diff}$ value increases during this immersion time and is $\sim 5.132$ kΩ. The corrosion products are partially deposited into the pores in the coating, and as a result, the further diffusion of the corrosion products

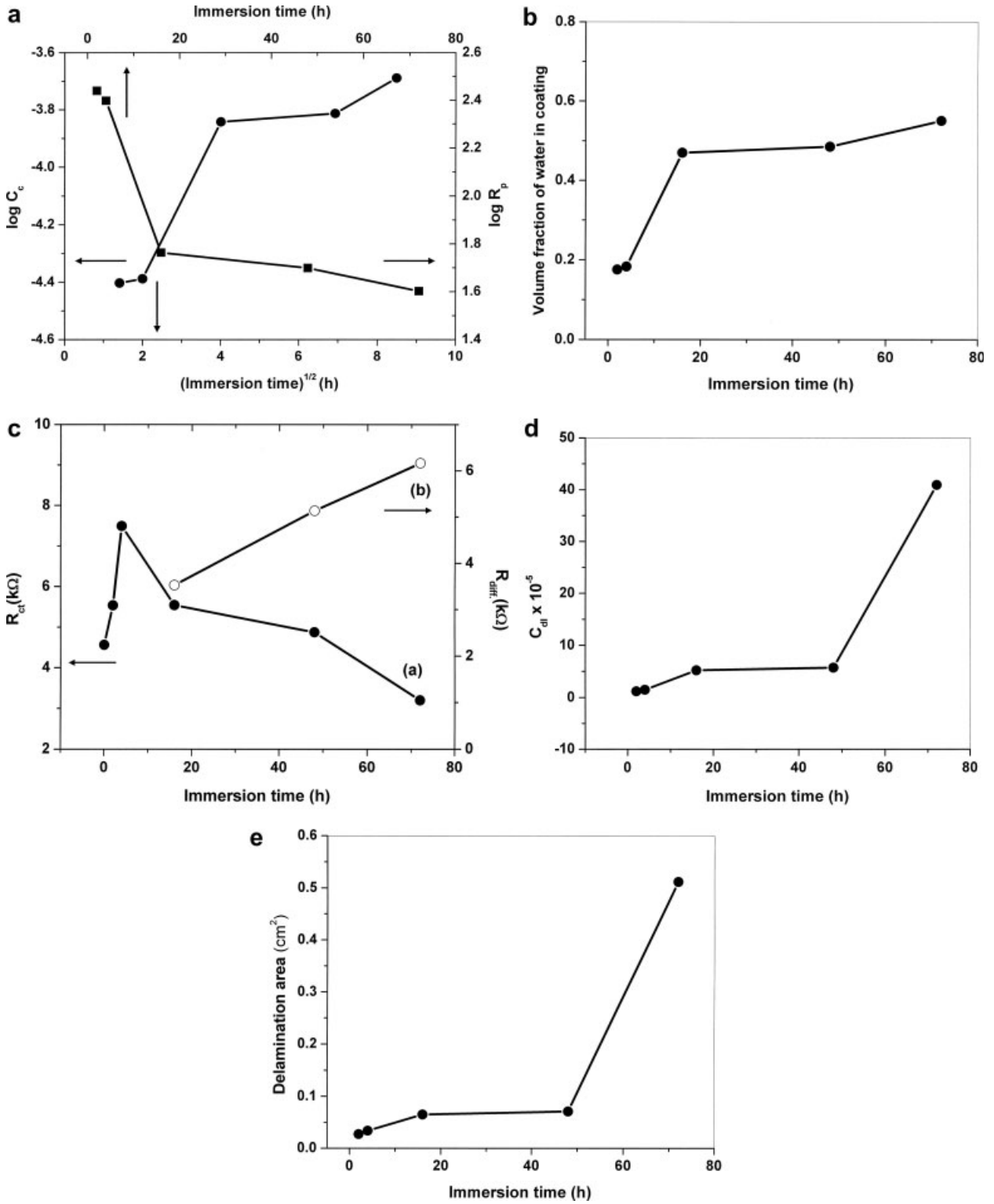


**Figure 6** (a) Evolution of $R_p$ and $C_c$ for POA-coated mild steel during exposure to 3% NaCl, (b) volume fraction of the electrolyte in the coating as a function of the immersion time in 3% NaCl, (c) evolution of $R_{ct}$ and $R_{diff}$ for POA-coated mild steel during exposure to 3% NaCl, (d) evolution of $C_{dl}$ for POA-coated mild steel during exposure to 3% NaCl, and (e) delamination area as a function of the immersion time in 3% NaCl.

toward the coating surface is hindered. Consequently, the increase in $R_{diff}$ can be observed during this immersion time.

The Nyquist impedance plot recorded after 72 h of exposure during immersion in an aqueous 3% NaCl solution is shown in Figure 5(e). After 72 h of

immersion time, a significant decrease in the $R_{ct}$ value can be observed, and its value is $\sim$ 3.199 k$\Omega$, which is still higher than that of the uncoated mild steel. As expected, the $R_{diff}$ value increases significantly, and its value is $\sim$ 6.163 k$\Omega$. During this immersion time, the diffusion of the corrosion products is hindered, and they accumulate at the bottom of the coating, resulting in the formation of a loose corrosion product layer.

After 96 h of immersion, the detachment in the coating was observed when the working electrode was removed from the test electrolyte, and so the immersion study was terminated at the end of 72 h.

### Evolution of the impedance parameters with the immersion time

The variation of $R_p$ as a function of the immersion time is shown in Figure 6(a). Initially, the value of $R_p$ decreases slowly, and this is attributed to the development of the electrolyte pathways through the POA coating. After 4 h of immersion, the $R_p$ value decreases sharply, and this reveals that the electrolyte has reached the mild steel surface.

$C_c$ is the capacitance of the intact coating layer or the capacitance of the areas in which rapid solution uptake does not occur.[38] The evolution of $C_c$ with the immersion time is also shown in Figure 6(a). As can be seen in Figure 6(a), the three time domains are clearly distinguished. First, a linear increase in $C_c$ can be observed during the first few hours, which is attributed to the entry of the electrolyte into the coating. This is the first step of the electrolyte penetration through the pores in the coating and is related to the water-uptake process. In the second domain, the coating is saturated with the water content, and the value of $C_c$ attains a plateau and remains constant over a long time period; this indicates the maintenance of the good protective properties due to the existence of the passive oxide layer. This is the second step of the electrolyte penetration and refers to the diffusion of water and ions via the pores in the coating. The corrosive species along with the water penetrates deeper and deeper with time until they finally pass through the POA coating and reach the mild steel surface. Finally, there is a rapid increase in $C_c$ over the third time domain, which indicates the onset of the corrosive processes at the surface of the mild steel and subsequently the detachment of the coating from the substrate due to adhesion loss.

The water uptake changes the dielectric constant of the polymer and therefore $C_c$. The volume fraction ($\phi$) of the water in the POA coating when in contact with a 3% NaCl solution as a function of time can be determined with the Brasher–Kingsbury equation:[39]

$$\phi = \frac{\log C_t/C_0}{\log 80}$$

where $C_t$ is the coating capacitance at instant $t$ and $C_0$ is the capacitance at $t = 0$. The value of 80 is the dielectric constant of water at 25°C. The volume fraction of water in the coating as a function of the immersion time is shown in Figure 6(b). The water permeation is very small up to 48 h of immersion, and this shows that the coating resists water uptake and is corrosion-resistant.

The variation of $R_{ct}$ as a function of the immersion time is shown in Figure 6(c). The $R_{ct}$ value increases up to 4 h of immersion and thereafter decreases with the immersion time; however, it is higher than that of the uncoated mild steel. The increase in the $R_{ct}$ value is attributed to the formation of protective oxide layers and the effective barrier behavior of the POA coating. After 16 h of immersion, the $R_{ct}$ value decreases with the increase in the immersion time; this reveals that the corrosion processes are initiated after 16 h of immersion.

The value of $R_{diff}$ increases [Fig. 6(c)] with the increase in the immersion time. As the immersion time increases, the amount of corrosion products formed at the interface of POA and the mild steel increases, and these products diffuse toward the coating surface. These corrosion products are deposited into the pores in the coating, and as a result, the further diffusion of the corrosion products toward the coating surface is hindered. Hence, the resistance against the diffusion of the corrosion products ($R_{diff}$) increases with the immersion time.

$C_{dl}$ represents the wet area under the coating, which is the area in contact with the electrolyte. The value of $C_{dl}$ increases linearly [Fig. 6(d)] during the first 16 h of immersion and thereafter remains almost constant. After 48 h of immersion, the $C_{dl}$ value increases sharply, and this indicates the increase in the wet area under the coating. The delamination area is evaluated by the comparison of the values of the measured $C_{dl}$ value with a specific capacitance $C_{dl}$ (measured on the uncoated substrate).[40] The determined delamination area values as a function of the immersion time [Fig. 6(e)] clearly indicate negligible delamination up to 48 h, as evident from the lowest values of the order of 0.027–0.071 cm$^2$. This confirms the stability of the POA coating on mild steel when exposed to a 3% NaCl solution.

## CONCLUSIONS

The performance of POA as a protective coating against the corrosion of mild steel was investigated through immersion tests performed in aqueous 3% NaCl solutions with EIS and open circuit potential measurements. The following main findings resulted from this investigation:

- The evolution of the equivalent circuit used to model the Nyquist impedance plot of the POA-coated steel with the immersion time was studied. During the initial period of immersion, the equivalent circuit modeling suggests that the impedance plot of the POA-coated steel can be fitted with two semicircles, which correspond to two time constants. It is suggested that the diffusion components related to the diffusion processes of corrosion products from the steel surface toward the coating must be considered in the equivalent circuit after a certain immersion time.
- After 16 h of immersion, the equivalent circuit fitting of the impedance plot of the POA-coated steel indicates that there are three semicircles, which correspond to three time constants.
- The water uptake and the delamination area were determined from the EIS study. The variation of the water uptake and delamination area with the immersion time provides further evidence of the protective action of POA.
- This study demonstrates that POA has excellent corrosion-protection properties and can be considered a potential coating material for the corrosion protection of mild steel in aqueous 3% NaCl.

## References


1. Song, H. K.; Palmore, G.; Tayhas, R. Adv Mater 2006, 18, 1764.
2. Cai, Z.; Geng, M.; Tang, Z. J Mater Sci 2004, 39, 4001.
3. Rosa, R. M.; Szulc, R. L.; Li, R. W. C.; Gruber, J. Macromol Symp 2005, 229, 138.
4. Sengupta, P. P.; Barik, S.; Adhikari, B. Mater Manufact Process 2006, 21, 263.
5. Wang, Y.; Jing, X. Polym Adv Technol 2005, 16, 344.
6. Jing, X.; Wang, Y.; Zhang, B. J Appl Polym Sci 2005, 98, 2149.
7. Lu, W.; Fadeev, A. G.; Qi, B.; Mattes, B. R. J Electrochem Soc 2004, 151, H33.
8. Srinivasan, S.; Pramanik, P. J Mater Chem 1994, 13, 365.
9. Pineri, M.; Schultze, J. W.; Vorotyntsev, M. A. Electrochim Acta 2000, 45, 2403.
10. Sexena, V.; Malhotra, B. D. Curr Appl Phys 2003, 3, 293.
11. Arulepp, M.; Permann, L. J Power Sources 2004, 133, 320.
12. Mansouri, J.; Burford, R. P. J Membr Sci 1994, 87, 23.
13. Bereket, G.; Hur, E.; Sahin, Y. Prog Org Coat 2005, 54, 63.
14. Herrasti, P.; Ocon, P.; Ibanez, A.; Fatas, E. J Appl Electrochem 2003, 33, 533.
15. Huerta-Vilca, D.; Siefert, B.; Moraes, S. R.; Pantoja, M. F.; Motheo, A. J. Mol Cryst Liq Cryst 2004, 415, 229.
16. Shinde, V.; Sainkar, S. R.; Patil, P. P. Corros Sci 2005, 47, 1352.
17. Shinde, V.; Sainkar, S. R.; Patil, P. P. J Appl Polym Sci 2005, 96, 685.
18. Zhang, T.; Zeng, C. L. Electrochim Acta 2005, 50, 4721.
19. Deberry, D. W. J Electrochem Soc 1985, 132, 1022.
20. Popovic, M. M.; Grgur, B. N. Synth Met 2004, 143, 191.
21. Martins, J. I.; Bazzaoui, M.; Reis, T. C.; Bazzaoui, E. A.; Martins, L. I. Synth Met 2002, 129, 221.
22. Bazzaoui, M.; Martins, L. I.; Bazzaoui, E. A.; Martins, T. I. Electrochim Acta 2002, 47, 2953.
23. Moraes, S. R.; Vilca, D. H.; Motheo, A. J. Prog Org Coat 2003, 48, 28.
24. Ogurtsov, N. A.; Pud, A. A.; Kamarchik, P.; Shapoval, G. S. Synth Met 2004, 143, 43.
25. Fenelon, A. M.; Breslin, C. B. Surf Coat Technol 2005, 190, 264.
26. Fenelon, A. M.; Breslin, C. B. Electrochim Acta 2002, 47, 4467.
27. Araujo, W. S.; Margarita, C. P.; Ferreira, M.; Mattos, O. R.; Neto, P. Electrochim Acta 2001, 46, 1307.
28. Iroh, J. O.; Su, W. Electrochim Acta 2000, 46, 15.
29. Lu, W. K.; Basak, S.; Elsenbaumer, R. L. In Handbook of Conducting Polymers, Skotheim, T. A.; Elsenbaumer, R.; Reynolds, J. R., Eds.; Marcel Dekker: New York, 1998; p 881.
30. Mattoso, L. H. C.; Bilhoes, L. O. S. Synth Met 1992, 52, 171.
31. Mattoso, L. H. C.; Manoher, S. K.; MacDiarmid, A. G.; Epstein, A. J. J Polym Sci Part A: Polym Chem 1995, 33, 1227.
32. Electrochemical Impedance Software: Z-Plot and Z-View; Scribner Associates: Southern Pines, NC, 2006.
33. Electrochemical Corrosion Software: CorrWare and CorrView; Scribner Associates: Southern Pines, NC, 2006.
34. Stillwell, D. E.; Park, S. M. J Electrochem Soc 1988, 135, 2254.
35. Tallman, D. E.; Pae, Y.; Bierwagen, G. P. Corrosion 2000, 56, 401.
36. Kousik, G.; Pitchumani, S.; Renganathan, N. G. Prog Org Coat 2001, 43, 286.
37. Zhang, T.; Zeng, C. L. Electrochim Acta 2005, 50, 4721.
38. Miskovic-Stankovic, V. B.; Drazic, D. M.; Teodorovic, M. J. Corros Sci 1995, 37, 241.
39. Brasher, D. M.; Kingsbury, A. H. J Appl Chem 1954, 4, 62.
40. Li, X. G. Haung, M. R.; Duan, W.; Yang, Y. L. Chem Rev 2002, 102, 2925.